Asian Journal of Chemistry; Vol. 32, No. 8 (2020), 1961-1966

ASIAN JOURNAL OF CHEMISTRY

https://doi.org/10.14233/ajchem.2020.22732

# Synthesis, Characterization and Ammonia Sensing Studies on Novel Polypyrrole/Zinc Oxide/SWCNT Nanocomposite

AHMAD HUSAIN[1], MOHD UROOJ SHARIQ[2,*], SHARIQUE AHMAD[1], ANEES AHMAD[2] and FAIZ MOHAMMAD[1]

[1]Department of Applied Chemistry, Faculty of Engineering and Technology, Aligarh Muslim University, Aligarh-202002, India
[2]Department of Chemistry, Faculty of Science, Aligarh Muslim University, Aligarh-202002, India

*Corresponding author: E-mail: murooj17@gmail.com

*Received*: 23 March 2020; *Accepted*: 8 May 2020; *Published online*: 27 July 2020; AJC-19974

Herein, the synthesis and characterization of a novel polypyrrole (PPy)/zinc oxide (ZnO)/SWCNT nanocomposite together with pristine polypyrrole is reported. These as-prepared materials have been characterized by FT-IR spectroscopy, X-ray diffraction (XRD), scanning electron microscopy (SEM), transmission electron microscopy (TEM) and thermogravimetric analysis (TGA) techniques. The PPy/ZnO/SWCNT nanocomposite is used as a pellet-shaped ammonia sensor. The sensing response is calculated in terms of variation in the DC electrical conductivity at different concentration of ammonia ranging from 50 ppm to 2000 ppm. The sensing response of the sensor is determined at 2000, 1000, 500, 400, 300, 200, 100 and 50 ppm and found to be 76.3, 60.5, 54.8, 52.6, 50.2, 48.5, 40.5 and 36.6%, respectively The sensor displays excellent reversibility along with very high selectivity and stability. Finally, a sensing mechanism is also proposed involving polarons (charge carriers) of polypyrrole and lone pairs of electrons of ammonia molecules.

**Keywords: Polypyrrole, Zinc oxide, SWCNT, Nanocomposite, Ammonia sensor.**

## INTRODUCTION

The discovery of conducting polymers by Shirakawa *et al.* [1] marked the beginning of a new era in the sphere of polymer science. Since, then the scientific community began to take an interest in the field of electrically conducting synthetic polymers. Ever since this branch of science has gathered impetus owing to a great deal of primary research been carried out. This field includes a variety of conjugated polymers such as polyacetylene, polypyrrole, polyaniline, polythiophenes and their nanocomposites, which have been used in sensing various gases/vapour/chemical [2-10]. These polymers are also termed as intrinsically conducting polymers (ICPs) as they possess native ability to conduct electricity *via* delocalization of charge through their extended $\pi$-conjugated system [3,7,8]. The sensors based on ICP respond very quickly to the analyte. But problems with these types of sensors are their poor stability, selectivity and reversibility [2]. These problems can be solved by preparing the nanocomposites of ICPs with inorganic nanomaterials like $SnO_2$, ZnO, graphene and carbon nanotubes, *etc*. The sensor-based on nanocomposites of ICPs exhibits outstanding sensing response, reversibility, selectivity and stability at room temperature as compared to pristine ICPs based sensors [3,6]. Amongst these ICPs, polypyrrole and their nanocomposites have shown a lot of promise commercially as it can be easily synthesized, is environmentally stable and possesses higher conductivity in comparison to the other ICPs available. Recently, many research papers have been published on gas/vapour sensors based on nanocomposites of polypyrrole [7-10].

In recent years, carbon nanotubes (CNT) have become indispensable building-blocks for sensing an assortment of gases as they possess excellent chemical stability, exceptional physical and chemical properties and high aspect ratio. The presence of these properties has opened up a broad range of applications for CNT, which include fabrication of nanoelectronic devices, chemical sensors, biosensors, *etc*. [11-13]. Gas sensors centred on PPy/CNT nanocomposites have engrossed massive interest in the past few years and they have been successful in detecting for ammonia [14].

Zinc oxide (ZnO) is an n-type semiconductor having a broad bandgap of 3.37 eV, and its exciton binding energy amounts to 60 meV. On account of these properties, ZnO nanomaterials display enhanced electron mobility. ZnO nanomaterials possess a high photoelectric reaction and are also chemically and thermally stable, which make them ideal contenders for fabricating functional chemical and biological sensors. ZnO-based nanostructures have received considerable attention in gas/vapour sensing applications recently. However to date, a large number of published reports are available for fabricating various types of sensing devices based on ZnO nanostructures, it remains a challenge for researchers to fabricate sensors which could be selective as well as sensitive [15,16].

Ammonia ($NH_3$), a harmful and poisonous gas is widely present in the environment in the form of vehicular exhausts and soils amended by urea. If inhaled in excess, it can lead to several health problems which include cough, difficulty in breathing, sore throat, tightness in the chest, tears, hoarse voice accompanied by dizziness, headache, nausea, vomiting, fatigue and various other symptoms. In some cases, exposure to large quantities of ammonia can lead to pulmonary edema and adult respiratory distress syndrome. Consequently, the development of a high-performance ammonia gas sensor operating at room temperatures and consuming less energy is extremely vital [7,10,17,18]. In this study, an effort to combine the unique properties of polypyrrole, ZnO and SWCNT to fabricate a novel pellet shaped ammonia sensor operating at room temperature is made. Polypyrrole (PPy) and PPy/ZnO/SWCNT nanocomposites were prepared by *in situ* chemical oxidative polymerization.

## EXPERIMENTAL

Pyrrole 99% (Sigma-Aldrich), anhydrous ferric chloride, methanol (Fischer Scientific India), zinc oxide nanoparticles and single-walled carbon nanotube (SWCNT) from Platonic Nanotech Limited Pvt Ltd. India was used as received. The water used in these experiments was double distilled.

**Synthesis of polypyrrole (PPy) and PPy/ZnO/SWCNT nanocomposite:** Polypyrrole (PPy) and PPy/ZnO/SWCNT nanocomposite were prepared by *in situ* oxidation polymerization method in aqueous medium using ferric chloride as oxidant [8,9]. In the preparation of PPy/ZnO/SWCNT nanocomposite, 100 mg SWCNT were added in 100 mL double distilled water and agitated for 30 min. After that 200 mg, ZnO was also added into the above mixture and sonicated for 1 h. Then 2.08 mL (0.03 mol) of pyrrole was added into the above suspension containing ZnO and SWCNT and sonicated for 3 h. Ferric chloride solution was prepared by adding 4.86 g (0.03 mol) of it into 100 mL double distilled water. After that ferric chloride solution was poured dropwise into the suspension of PPy, ZnO and SWCNT with continuous stirring. After 12 h a black coloured slurry was obtained which was washed and filtered using double distilled water and methanol. The filtered material (nanocomposites) was dried in an air oven at 70 ºC for 24 h. Thus synthesized nanocomposite was named as PPy/ZnO/SWCNT. The pristine PPy was also prepared by an identical method in the absence of ZnO and SWCNT.

**Characterization:** Fourier transform infrared spectroscopy (FTIR) spectra were recorded using Perkin-Elmer 1725 instrument on KBr pellets. To conduct morphological studies scanning electron microscopy (SEM) and transmission electron microscopy (TEM) was done using JEOL, JSM, 6510-LV (Japan) and JEM 2100, JEOL (Japan), respectively. X-ray diffraction (XRD) data were recorded by Bruker D8 diffractometer with Cu*K*α radiation at 1.540 Å in the range of $5° \leq 2\theta \leq 80°$ at 50 kV. The thermogravimetric analysis (TGA) was performed by Perkin-Elmer (Pyris Dimond) instrument, heating the samples from 24 ºC to 1000 ºC at the rate of 10 ºC $min^{-1}$ in nitrogen atmosphere at the flow rate of 200 mL/min.

## RESULTS AND DISCUSSION

**FT-IR studies:** Fig. 1 shows the FTIR spectra of PPy and PPy/ZnO/SWCNT nanocomposite. The characteristic peaks of PPy at 3388, 1550, 1310, 1192, 1088 and 1044 $cm^{-1}$ is attributed to N-H stretching, C=C stretching, C=N bending, C-N stretching and =C-H bending, respectively as shown in Fig. 1a. [8,9]. The band at 920 $cm^{-1}$ corresponds to the $C=N^{+}$-C stretching and has been accredited to the formation of polarons (charge carriers), which is also supportive of their doping by $FeCl_3$. This result also confirms that polypyrrole was oxidized by $FeCl_3$ containing positively charged entities, *i.e.* polarons [8,9]. The slight decrease in the N-H, C=C, C=N and C-N stretching frequencies in the spectra of PPy/ZnO/SWCNT nanocomposite (Fig. 1b) may be owing to the interaction of ZnO nanoparticles and SWCNT with PPy backbone. In the case of PPy/ZnO/SWCNT nanocomposites, the slight shift in the positions of characteristic peaks of PPy confirms the successful formation of nanocomposite in which ZnO and SWCNT are covered by the matrix of PPy as revealed by SEM and TEM microscopy.

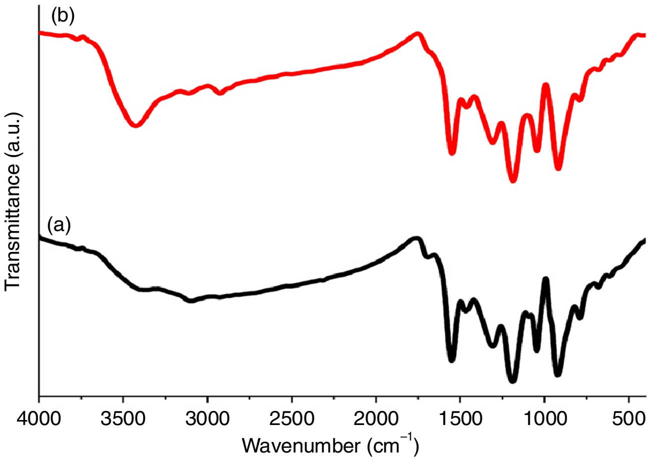

Fig. 1. FT-IR spectra of (a) PPy and (b) PPy/ZnO/SWCNT nanocomposite

**X-ray diffraction study:** Fig. 2 represents the X-ray diffraction patterns of PPy and PPy/ZnO/SWCNT nanocomposites. A broad peak observed at $2\theta = 24.7°$, represents the repeating units of pyrrole ring, confirming the amorphous nature of PPy as shown in Fig. 2a [8,9]. The main characteristic peaks of ZnO nanoparticles in PPy/ZnO/SWCNT nanocomposite were observed at $2\theta$ = 33.27º, 35.67º, 54.10º, 62.38º, 64.20º as shown in Fig. 2b, which correspond to the (002), (101), (110), (103) and (200) planes of ZnO nanoparticles, respectively [19]. In case of PPy/ZnO/SWCNT nanocomposite, the broadening and shifting of characteristic peaks of PPy (at $2\theta = 24.9°$) confirms

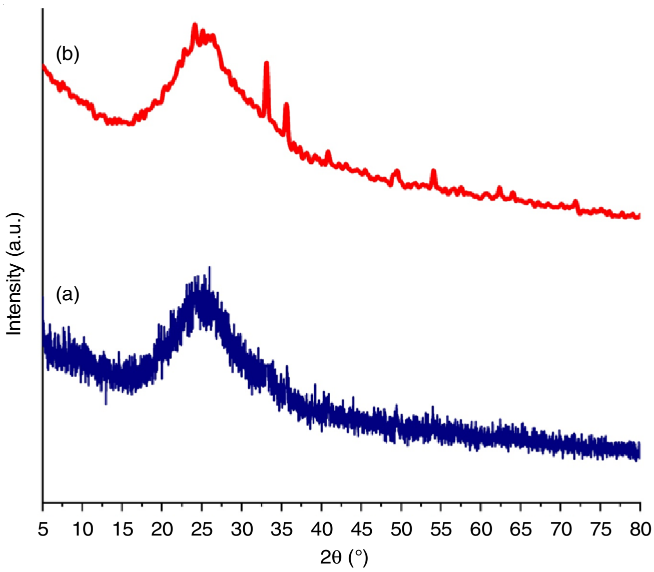

Fig. 2. XRD spectra of (a) PPy and (b) PPy/ZnO/SWCNT nanocomposite

the interaction of PPy with the ZnO and SWCNT which is also supported by FTIR results.

**Scanning electron microscopy (SEM) studies:** The surface morphology of PPy and PPy/ZnO/SWCNT nanocomposite was revealed by SEM micrographs as shown in Fig. 3. The morphology of pristine PPy (Fig. 3a) shows the agglomeration of several globular nanoparticles. In the case of PPy/ZnO/SWCNT nanocomposite, a slight change in morphology is observed and globular nanoparticles become larger in size (Fig. 3b). There are no free ZnO nanoparticle and SWCNT which confirms the polymerization of pyrrole on the surface of ZnO nanoparticle and SWCNT. However, there is a linear structure decorated with some globular nanoparticles (enclosed in the marked circle), which is due to entrapment of SWCNT as well as ZnO nanoparticle inside the PPy matrix due to electronic interaction of PPy chains with both the ZnO nanoparticle and SWCNT.

**Transmission electron microscopy (TEM) studies:** The TEM micrographs of PPy/ZnO/SWCNT nanocomposite at two different magnification *viz.* 100 nm and 50 nm are given in Fig. 4. These micrographs revealed an encapsulation of ZnO nanoparticles (dark black coloured) and SWCNT into the matrix of PPy (grey coloured part). The decoration of ZnO nanoparticles on SWCNT can be observed on which polymerization of pyrrole takes place. Thus, the formation of PPy chain on the vast surface area of ZnO nanoparticles on SWCNT provides a large number of adsorption sites, which is very advantageous in the sensing.

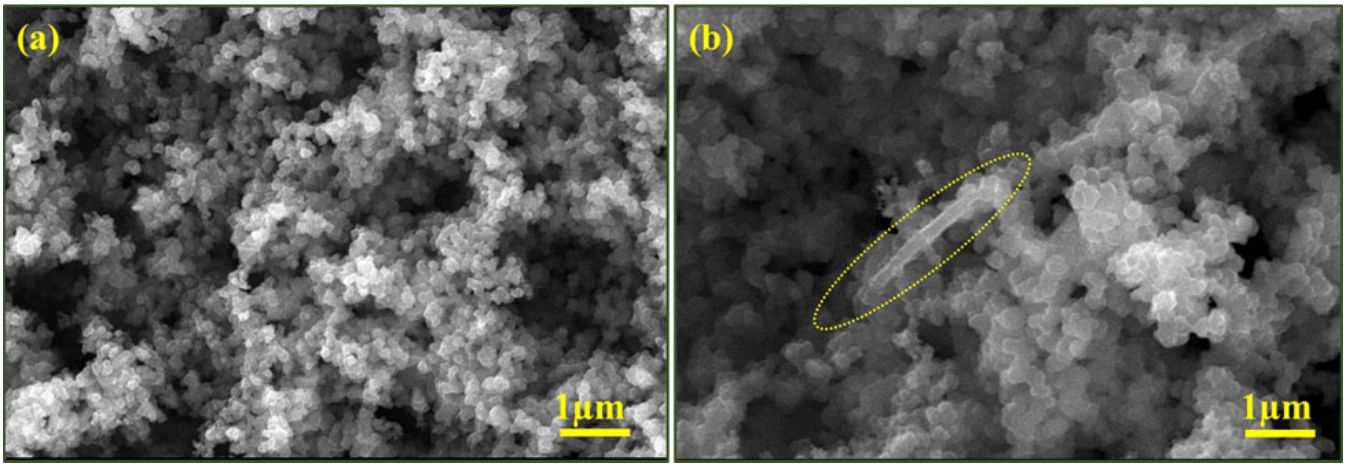

Fig. 3. SEM micrographs of (a) PPy and (b) PPy/ZnO/SWCNT nanocomposite

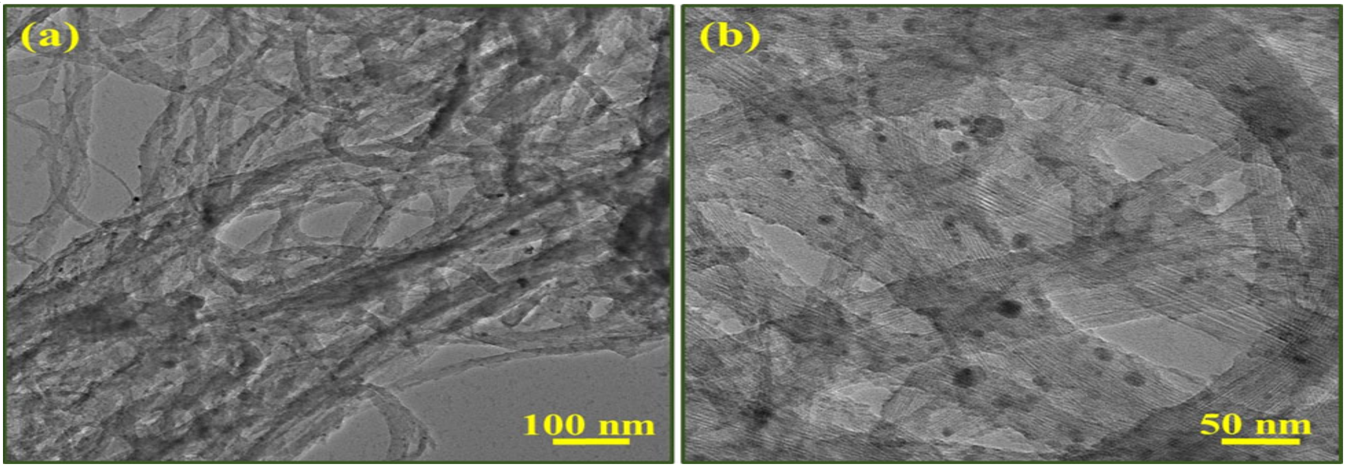

Fig. 4. TEM micrographs PPy/ZnO/SWCNT nanocomposite at different magnifications

**Thermogravimetric analysis:** Fig. 5 represents the TGA thermographs of PPy and PPy/ZnO/SWCNT nanocomposites. The weight loss% and thermal stability of PPy and PPy/ZnO/SWCNT nanocomposite were determined by TGA technique in the range of 30-600 ºC. In case of PPy (Fig. 5a), there were three weight loss processes at about 80 ºC, 270 ºC and 360 ºC, which may be related to the removal of moisture, loss of dopant and degradation of polymer chain, respectively [9]. In case of PPy/ZnO/SWCNT nanocomposites (Fig. 5b), the weight loss process started at about 400 ºC, which showed the greater thermal stability of it as compared to pristine PPy. At 600 ºC, the weight loss% was 81.60% and 25.94% for PPy and PPy/ZnO/SWCNT nanocomposites, respectively. Thus, the outstanding thermal stability of PPy/ZnO/SWCNT nanocomposites confirmed the formation of nanocomposite due to a strong electronic interaction of PPy chain with ZnO nanoparticle and SWCNT.

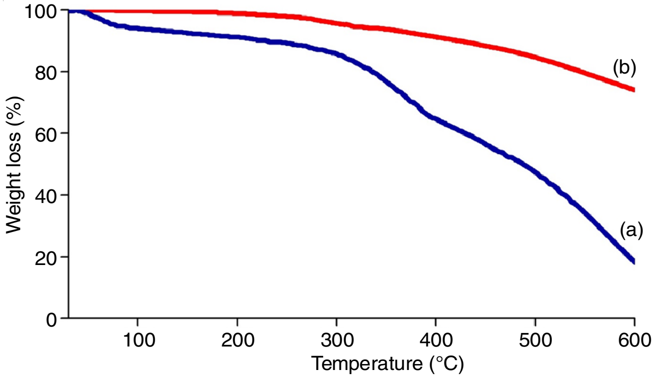

Fig. 5. Thermograms of (a) PPy and (b) PPy/ZnO/SWCNT nanocomposite

**Sensing:** For performing the ammonia sensing experiments, 0.350 g of PPy/ZnO/SWCNT nanocomposite was converted into pellet-shaped sensing material by applying a pressure of 75 kN applied for 15 min using a hydraulic machine. The sensing experiments of PPy and PPy/ZnO/SWCNT nanocomposites were performed by using a four-in-line probe with a temperature controller (PID-200, Scientific Equipments, India). All the sensing experiments were carried out at room temperature. The DC electrical conductivity was calculated using the following equation:

$$\sigma = \frac{[\ln 2(2S/2)]}{[2\pi S(V/I)]} \qquad (1)$$

where I, V, W and S stand for the current (A), voltage (V), thickness of the pellet (cm) and probe spacing (cm), respectively and σ is the conductivity (S cm$^{-1}$) [20,21].

**Sensing response:** The sensing response (%) of the sensor was calculated as the function of change in DC electrical conductivity in the exposure of ammonia vapour for 60 s. The formula used for the calculation of % sensing response (S) was as follows:

$$S = \frac{\Delta\sigma}{\sigma_i} \times 100 \qquad (2)$$

where: $\sigma_i$ and Δσ represent the initial DC electrical conductivity and change in DC electrical conductivity in the exposure of ammonia for 60 s, respectively [20].

First of all, the sensor-pellet was properly attached to the four-in-line probe of the device. Then, the probe was kept in the sealed beaker containing highly volatile ammonia solution of known concentration for 60 s. In the exposure of ammonia vapour, the conductivity of the sensor started to decrease till 60 s. During this period of 60 s, the change in conductivity was calculated for determining the sensing response. After that, the probe holding sensor-pellet was removed from the beaker containing ammonia solution and exposed in the fresh air for 60 s. The conductivity started to increase in air and returned to near its initial value after 60 s (Fig. 6).

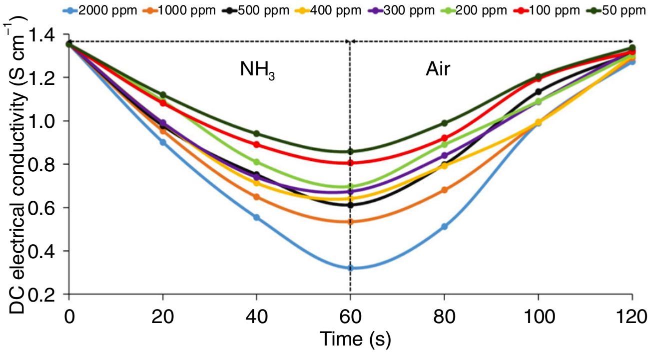

Fig. 6. Variation in DC electrical conductivity of sensor on alternate exposure of ammonia and air at different concentrations

In the presence of ammonia vapour, a decrease in the conductivity is due to the interaction of lone pairs of electrons of nitrogen atoms of ammonia molecules with the charge carriers (holes) of PPy. In case of conducting polymers like polypyrrole, polythiophene and polyaniline, *etc*. the charge carriers are polarons and bipolarons which act as a hole. The electrical conductivity is directed by the number of these charge carriers (holes) besides their mobility along with the extended π-conjugated structure. Thus, any interaction which neutralize or reduces the mobility of these charge carriers can alter the electrical conductivity of PPy [4,5,8,9]. As we know that ammonia is a good Lewis base, which easily donates its lone pair to positively charged holes of PPy. There may be two possibilities when ammonia molecules get adsorbed on the sensor surface; (i) complete neutralization of charge carriers due to donation of lone pair of electrons of ammonia to the charge carriers (holes) of PPy and (ii) the weak electronic interaction between lone pairs of electrons and charge carriers (holes) of PPy.

In this study, second type interaction is possible only because the sensor showed a dynamic response in conductivity, *i.e.* decrease in ammonia vapour and then returned to its original value in air. This is due to desorption of ammonia molecules from sensor surface in the air and thus deletion of electronic interaction between lone pairs of electrons and charge carriers of PPy.

The sensing response of sensor was calculated at 2000, 1000, 500, 400, 300, 200, 100 and 50 ppm and found to be 76.3, 60.5, 54.8, 52.6, 50.2, 48.5, 40.5 and 36.6%, respectively (Fig. 7). Greater sensing response at higher concentration is due to the availability of a larger number of ammonia molecules (*i.e.* greater number of lone pairs), which reduce the mobility of a huge number of charge carriers. Thus, greater change in

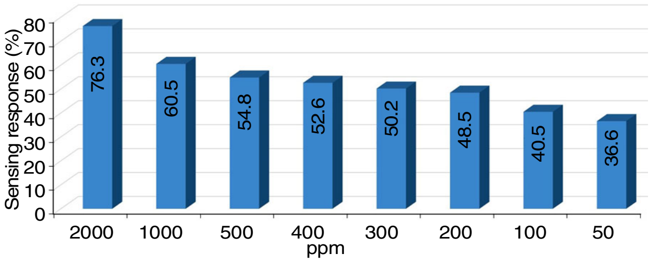

Fig. 7. Sensing response of the sensor towards ammonia at different concentrations

conductivity (*i.e.* sensing response) was observed at higher concentration. On the other hand, the change in conductivity was minor due to a reduction in the mobility lesser number of charge carriers by comparably lesser number of lone pairs of ammonia at lower concentrations. The results show that the sensor can detect ammonia vapour at very low concentration of 50 ppm with a sensing response of 36.6%.

**Reversibility:** The reversibility of the sensor was studied by exposing the sensor-pellet in ammonia vapour for 30 s. Then, sensor-pellet was removed from ammonia vapour and exposed in the air for 30 s. These procedures were followed for three continuous cycles comprising of total 180 s as shown in Fig. 8. The sensor shows an excellent dynamic response, *i.e.* decrease and recovery of initial conductivity in the ammonia vapour and air, respectively, revealing a highly reversible nature of the sensor. After three complete cycles, the conductivity did not return to the initial value at 2000 ppm and 1000 ppm due to partial desorption of ammonia molecules from the sensor surface. But at a lower concentration, the initial conductivity recovered completely due to complete desorption of the lesser number of adsorbed ammonia molecules from the sensor surface. Thus, this ammonia sensor exhibits complete reversibility at lower concentrations *viz.* 300, 200, 100 and 50 ppm.

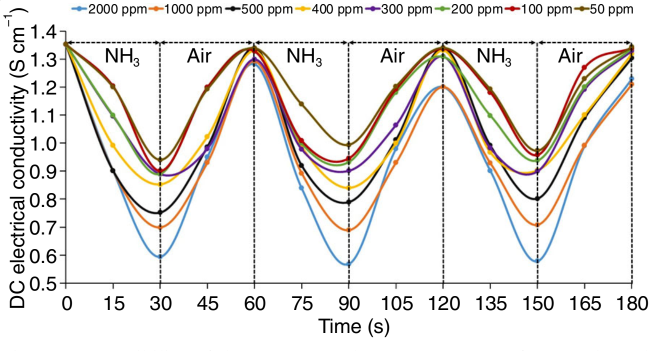

Fig. 8. Reversibility of the sensor on alternate exposure of ammonia and air at different concentrations

**Selectivity:** The selectivity of the sensor towards ammonia vapour was determined in the exposure of some common volatile organic compounds (VOCs), *e.g.* ethanol, methanol, acetone and acetaldehyde at the highest and the lowest concentrations, *i.e.* at 2000 ppm and 50 ppm, respectively (Fig. 9). The sensor pellet was exposed in ammonia and all the tested VOCs one by one for 60 s and then the sensing response was calculated. At 2000 ppm, the sensing response was found to be 76.3, 23.1, 21.4, 14.3 and 9.2% towards ammonia, ethanol, methanol, acetone and acetaldehyde, respectively. So, even at a higher concentration of 2000 ppm, the sensor showed high selectivity. Whereas at 50 ppm, the sensor responded towards ammonia only with a sensing response of 36.6%. Therefore, the sensor was found to be exclusively selective for ammonia vapour at 50 ppm.

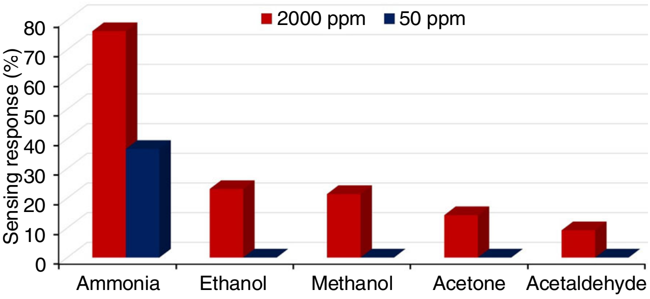

Fig. 9. Selectivity of the sensor at 2000 ppm and 50 ppm of ammonia

**Stability:** The stability of sensor operating at room temperature is considered to be an important constraint for practical application. The major concern of the sensors based on conducting polymers is their poor stability. The sensitivity of these sensors drastically reduces after some days. However, the stability of the sensors based on nanocomposites of conducting polymers is much improved as compared to pristine polymers due to the outstanding stability of filler inorganic nanomaterials [3,6,10].

In this study, the stability was determined by calculating the sensing response for consecutive 15 days at the lowest and the highest concentrations, *i.e.* 50 and 2000 ppm concentrations of ammonia (Fig. 10). The sensor exhibited excellent stability even after 15 days at both the tested concentrations.

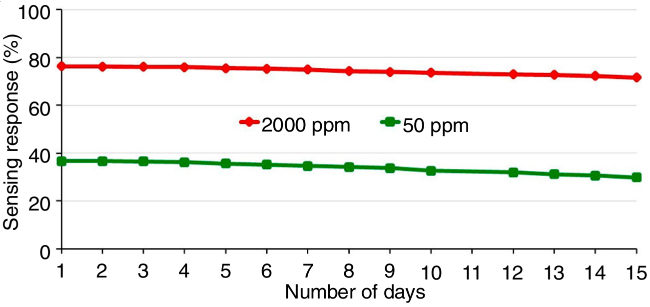

Fig. 10. Stability of the sensor at 2000 ppm and 50 ppm of ammonia

**Sensing mechanism:** In case of the sensors based on the conducting polymers, adsorption of the analyte gas/vapour on the sensor surface is supposed to the very first step. After adsorption, analyte molecules interact with the charge carriers (polarons/bipolarons) of the polymer affecting alteration in the electrical properties (resistance/conductivity). However, this process is found to be more robust in conducting polymer-based nanocomposites. The reversible nature of the sensor is due to desorption of analyte molecules from sensor surface when exposed in the air [4,5,8,9,20,21].

In this study, we have proposed the sensing mechanism based on adsorption/desorption phenomena of ammonia molecules on the vast surface area of sensor-pellet (Fig. 11). Ammonia is an electron-rich molecule and good Lewis base. The lone pairs of electrons of the adsorbed ammonia molecules

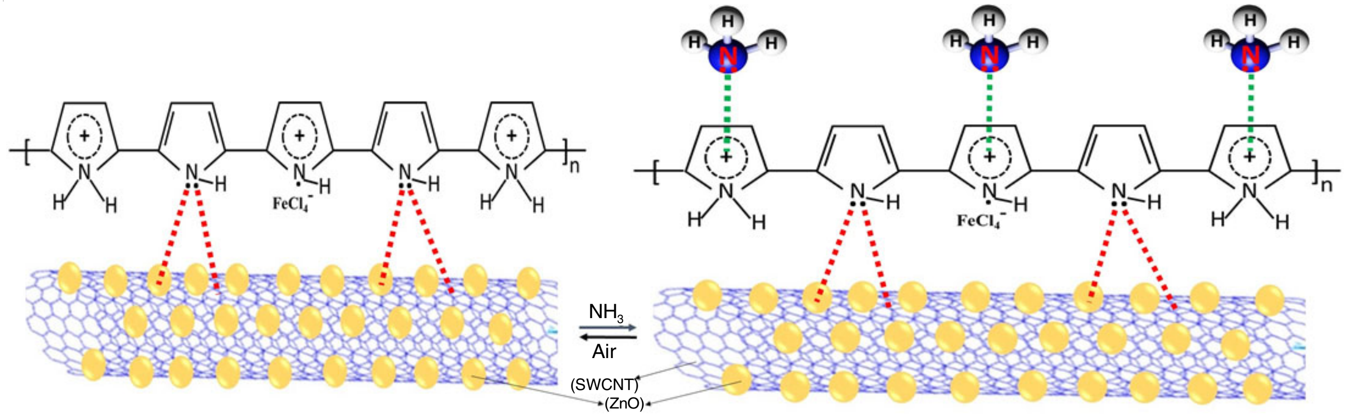

Fig. 11. Proposed sensing mechanism concerning the electronic interaction of charge carriers of PPy with lone pairs of ammonia molecules

interact at the electron-deficient charge carriers (holes) of PPy which reduces the charge intensity and mobility of the charge carriers. Therefore, a sudden decrease in conductivity was observed as soon as sensor-pellet got exposed in ammonia vapour. When sensor-pellet was exposed in air, desorption of ammonia molecules started resulting in an increase in conductivity. After complete desorption of ammonia molecules from the sensor, the charge intensity and mobility of charge carriers recovered, leading to the retrieval of initial DC electrical conductivity of the sensor.

## Conclusion

In this study, *in-situ* oxidative polymerization method for the preparation of a novel PPy/ZnO/SWCNT nanocomposite in aqueous medium using ferric chloride as an oxidant is used. The structure and morphology of the prepared material were studied by FT-IR spectroscopy, X-ray diffraction technique, scanning electron microscopy, transmission electron microscopy and thermogravimetric analysis. The PPy/ZnO/SWCNT nanocomposite has been used to fabricate a pellet-shaped ammonia vapour sensor operating at room temperature. The sensing response of the sensor was found to be 76.3, 60.5, 54.8, 52.6, 50.2, 48.5, 40.5 and 36.6% at 2000, 1000, 500, 400, 300, 200, 100 and 50 ppm of ammonia, respectively. The sensor was found to be completely reversible as well as very stable till 15 days. The sensor shows high selectivity towards ammonia at 2000 ppm, but at 50 ppm it is exclusively selective, *i.e.* responds to ammonia only in the presence of different VOCs tested. Thus, PPy/ZnO/SWCNT nanocomposite can be used to fabricate highly efficient and novel ammonia vapour sensor at room temperature.

## ACKNOWLEDGEMENTS

The authors would like to acknowledge Noohul Alam (Research Scholar, Indian Institute of Technology Patna, India) for helpful discussions.

## CONFLICT OF INTEREST

The authors declare that there is no conflict of interests regarding the publication of this article.

## REFERENCES

1. H. Shirakawa, E.J. Louis, A.G. MacDiarmid, C.K. Chiang and A.J. Heeger, *J. Chem. Soc. Chem. Commun.*, 578 (1977); https://doi.org/10.1039/c39770000578
2. H. Bai and G. Shi, *Sensors (Basel)*, **7**, 267 (2007); https://doi.org/10.3390/s7030267
3. Rajesh, T. Ahuja and D. Kumar, *Sens. Actuators B Chem.*, **136**, 275 (2009); https://doi.org/10.1016/j.snb.2008.09.014
4. A. Husain, S. Ahmad and F. Mohammad, *Mater. Today Commun.*, **20**, 100574 (2019); https://doi.org/10.1016/j.mtcomm.2019.100574
5. A. Husain, S. Ahmad and F. Mohammad, *Mater. Chem. Phys.*, **239**, 122324 (2020); https://doi.org/10.1016/j.matchemphys.2019.122324
6. S. Pandey, *J. Sci. Adv. Mater. Devices*, **1**, 431 (2016); https://doi.org/10.1016/j.jsamd.2016.10.005
7. M. Šetka, J. Drbohlavová and J. Hubálek, *Sensors*, **17**, 562 (2017); https://doi.org/10.3390/s17030562
8. A. Sultan, S. Ahmad and F. Mohammad, *RSC Adv.*, **6**, 84200 (2016); https://doi.org/10.1039/C6RA12613H
9. A. Sultan, S. Ahmad and F. Mohammad, *Polym. Polymer Compos.*, **25**, 695 (2017); https://doi.org/10.1177/096739111702500908
10. A. Beniwal and Sunny, *Sens. Actuators B Chem.*, **296**, 126660 (2019); https://doi.org/10.1016/j.snb.2019.126660
11. K.S. Ibrahim, *Carbon Lett.*, **14**, 131 (2013); https://doi.org/10.5714/CL.2013.14.3.131
12. S. Kumar, V. Pavelyev, P. Mishra and N. Tripathi, *Sens. Actuators A Phys.*, **283**, 174 (2018); https://doi.org/10.1016/j.sna.2018.09.061
13. N. Van Hieu, L.T.B. Thuy and N.D. Chien, *Sens. Actuators B Chem.*, **129**, 888 (2008); https://doi.org/10.1016/j.snb.2007.09.088
14. N. Van Hieu, N.Q. Dung, P.D. Tam, T. Trung and N.D. Chien, *Sens. Actuators B Chem.*, **140**, 500 (2009); https://doi.org/10.1016/j.snb.2009.04.061
15. A. Wei, L. Pan and W. Huang, *Mater. Sci. Eng. B Solid-State Mater. Adv. Technol.*, **176**, 1409 (2011); https://doi.org/10.1016/j.mseb.2011.09.005
16. L. Zhu and W. Zeng, *Sens. Actuators A Phys.*, **267**, 242 (2017); https://doi.org/10.1016/j.sna.2017.10.021
17. B. Timmer, W. Olthuis and A. Berg, *Sens. Actuators B Chem.*, **107**, 666 (2005); https://doi.org/10.1016/j.snb.2004.11.054
18. D. Kwak, Y. Lei and R. Maric, *Talanta*, **204**, 713 (2019); https://doi.org/10.1016/j.talanta.2019.06.034
19. S. Talam, S.R. Karumuri and N. Gunnam, *Int. Schol. Res. Notices*, **2012**, 372505 (2012); https://doi.org/10.5402/2012/372505
20. A. Husain, M.U. Shariq and F. Mohammad, *Materialia*, **9**, 100599 (2020); https://doi.org/10.1016/j.mtla.2020.100599
21. A. Husain, S. Ahmad and F. Mohammad, *J. Sci. Adv. Mater. Devices,* **5**, 84 (2020); https://doi.org/10.1016/j.jsamd.2020.01.002